Dynamics of Magnetic Bubbles in Acoustic and Magnetic Fields

Xue Zhao, Pedro A. Quinto-Su, and Claus-Dieter Ohl

Division of Physics and Applied Physics, School of Physical and Mathematical Sciences, Nanyang Technological University, Singapore 637371, Singapore

(Received 24 June 2008; published 16 January 2009)

We report on shelled bubbles that can be manipulated with magnetic fields. The magnetic shell consists of self-assembled magnetic nanoparticles. The magnetic susceptibility of the bubbles is proportional to the surface area, $\chi_b = (9 \pm 3 \times 10^{-6}\ \mathrm{m})r^2$ where r is the radius. Magnetic bubbles are compressible in moderate acoustic fields. A bubble with a radius of 121 μm oscillates in resonance in a sound field of 27 kHz with a peak-to-peak radial amplitude of 1.7 μm. The bubble oscillations induce a microstreaming flow with a toroidal vortex at the upper pole of the bubble. Further findings are the longevity of the magnetic bubbles and the ease of manipulation with standard magnets.

DOI: 10.1103/PhysRevLett.102.024501 PACS numbers: 47.55.dd, 41.20.Gz, 47.35.Rs

Bubbles in liquids driven by a sound field are used in many disciplines: for example, they clean surfaces [1] in ultrasonic water baths, and they catalyze unique chemical reactions in sonochemistry [2,3]. Shelled micrometer sized bubbles reflect diagnostic ultrasound [4] and allow pictures of organ perfusion [5] or cancerous tumors [6] to be taken. Recently, bubbles have been engineered to bind to certain cell types [7], to deliver medication, or to serve as a viral surrogate for gene therapy [8]. Here we report on bubbles with a magnetic moment due to a shell of self-assembled nanoparticles. We characterize their magnetic properties and demonstrate that they oscillate in an acoustic field. Some previous work has reported on very small bubbles with a magnetic shell for medical use [9] using either electrostatic coupling or water-oil emulsions to attach the nanoparticles to the bubble surface. Neither their magnetic properties nor their response to an acoustic field has been measured. In contrast our new and simple recipe allows the creation of much larger and stable bubbles which we now characterize physically.

In an acoustic field, conventional free and also shelled bubbles experience two forces: a surface force compressing and expanding the gas, and additionally a radiation force caused by spatial gradients of the pressure field, the so-called Bjerknes force [10]. This Bjerknes force accelerates the bubbles into translational motion which makes it very difficult and sometimes impossible to control their oscillations and position simultaneously. An exceptional example is single bubble sonoluminescence [11] where a single bubble is trapped in the field due to the balance between buoyancy and Bjerknes force. Prior successful attempts to affect bubbles' oscillations with magnetic fields implemented complex and costly experimental equipment [12] due to the low magnetic susceptibility of water. In contrast, the magnetic shelled bubbles reported here possess sufficient magnetization such that they can be controlled with conventional magnets, and their shell elasticity still allows for volume oscillations in moderate acoustic fields. In this Letter we first describe the recipe to create the bubbles, then we image them using an optical microscope, and the shells magnetic susceptibility is measured with a force balance model. Finally, we show the compressibility of the bubbles in moderate acoustic fields, which leads to a microstreaming flow. These observations show the great potential that magnetic bubbles have for a wide range of applications, as the bubbles can be manipulated with magnetic and acoustic fields.

The magnetic bubbles are prepared using a simple procedure that involves self-assembly of magnetic nanoparticles: Magnetite nanoparticles were prepared in open air at room temperature. We added 4.2 mL of 1 M KOH aqueous solution to 25 mL of 0.1 M $FeCl_2$ aqueous solution. Then 250 μL of H_2O_2 3 wt % aqueous solution was added into the solution to yield a black precipitate. The particles were separated by magnetic decantation, washed 3 times with 20 mL distilled water, 2 times with 20 mL acetone, and finally dried in air at room temperature. Presumably the structure of the nanoparticles [13] is an intermediate between Fe_3O_4 and γ-Fe_2O_3. Eight milligrams of the magnetic nanoparticles were washed with 4 mL ultrapure water once, dispersed in 4 mL ultrapure water, and sonicated for ten minutes to obtain a uniform black solution. Next 500 μL of 5 mM of the surfactant sodium dodecyl sulfate was added to 500 μL of the solution, and then shaken moderately for three minutes to form the magnetic bubbles.

Viewing the bubbles under a microscope reveals their metallic appearance, which is caused by a thin shell of metallic nanoparticles [13]. In Fig. 1, the bubbles have been pipetted onto a glass slide. There, they rise to the top of the water droplet where they are imaged from above with a 5× objective. The thickness of the shell has been explored with scanning electron microscopy after the bubbles have been air dried; an example of the cross section of the shell is shown in the inset of Fig. 1. The shell thickness after drying is about 880 nm for bubbles with radii in the range of 50 to 175 μm. The scanning electron microscopy images reveal that the distribution of grains of magnetic material is not very uniform.

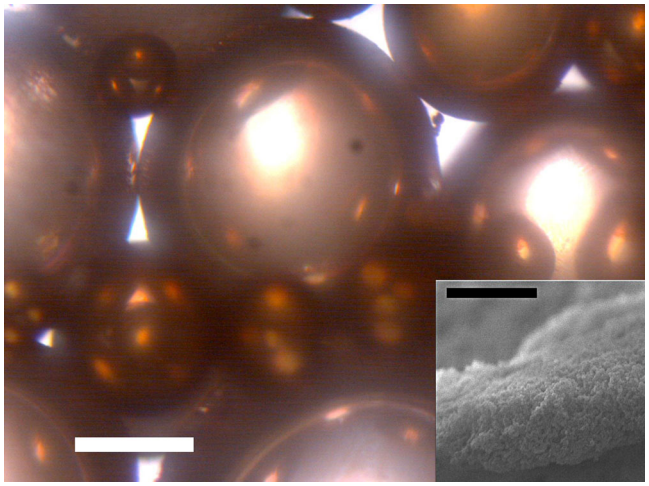

FIG. 1 (color online). Microscopic view of magnetic bubbles. The Christmas-tree-ball-like appearance of the magnetic bubbles is due to a thin layer of metallic nanoparticles (length of the scale bar 300 μm). The inset shows a cross section of the shell taken with a scanning electron microscope (length of the scale bar 1 μm).

Interestingly, the bubbles are very stable in gas-saturated water: a sample of magnetic shelled bubbles remained intact for more than six months in a light tight lab drawer. However, when bubbles are pipetted from gas-saturated water into degassed water, they lose buoyancy and sink to the bottom. As an example, we measured a dissolution time of 700 s for a magnetic bubble with an initial radius of 148 μm in water at 35% of saturation concentration of O_2. Comparing this time with the solution of the diffusion equation (see, for example, [14]) for a free bubble we find an increase of 2.3 times in the dissolution time which can be explained by the hindrance of the diffusion by the porous shell of the magnetic bubbles. This observation is also supported by the fact that bubbles heated in gas-saturated water expand. Thus the shell of the magnetic bubble is gas permeable. The longevity of the bubbles in saturated water indicates that the arrangement of the nanoparticles in the shell is stable. In contrast, free bubbles eventually dissolve due to the Laplace pressure.

To measure the magnetic properties of the bubbles we used the experimental setup shown in Fig. 2(a). We let a bubble rise to the air-water interface in a transparent container; then a permanent Nd magnet is brought from below towards the container in small increments until the magnetic force overcomes buoyancy [Fig. 2(a)] and the bubble sinks to the bottom. To obtain an expression for the magnetic force [15] acting on the bubble we neglect all field gradients except the one along the y axis. Then the magnetic force in the y direction is $F_{\mathrm{mag}} = \chi_b \mu_0^{-1} B dB/dy$, where B is the magnitude of the magnetic field, μ_0 is the permeability of vacuum, and χ_b is the magnetic susceptibility of the bubble (in units of volume). The bubble's trajectory is recorded with a digital camera (model EO-

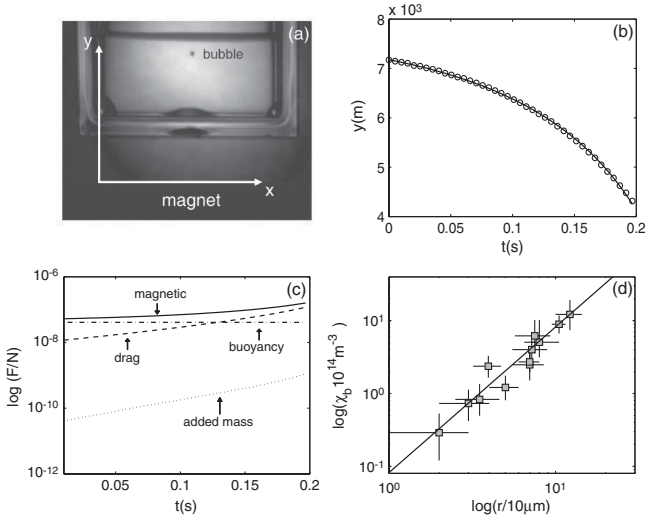

FIG. 2. (a) Experimental setup for measuring the bubble trajectory. (b) Bubble trajectory for a $r = 100$ μm bubble (circles) and fit to model (solid line). (c) Forces acting on the bubble as it sinks to the bottom of the container: magnetic (solid line), buoyancy (dash-dotted line), drag (dashed line), and added mass (dotted line). (d) Extracted magnetic susceptibility χ_b from a force balance model fitted to the measured trajectories (see text) and plotted as a function of radius double logarithmically. The error bars account for the uncertainty in bubble radius, its trajectory, and the magnetic field.

1312M, Edmund Optics, NJ, USA) and modeled with Newton's 2nd law, by balancing the magnetic, buoyancy, drag, and added mass force [16]:

$$-\frac{1}{2}\frac{d^2y}{dt^2}V_B\rho_w - \frac{1}{2}\rho_w \pi r^2 C_d \frac{dy}{dt}\left|\frac{dy}{dt}\right| + \rho_w V_B g + \frac{\chi_b}{\mu_0} B \frac{dB}{dy} = 0. \quad (1)$$

The first term represents the added mass force due to the fluid displaced by the bubble, and the second term is the drag force, followed by buoyancy, and the magnetic force. The volume and radius of the bubble are V_B and r, respectively. Further constants are the density of the liquid $\rho_w = 10^3$ kg/m^3 and the acceleration of gravity g. The Reynolds number is defined as $\mathrm{Re} = |\frac{dy}{dt}|r/\nu$, where $\nu = 10^{-6}$ m^2/s is the kinematic viscosity of water. For the experiments presented here the Reynolds number ranges between 0 and 10. Therefore, a correction to the standard Stokes drag law is applied [17]; thus, the drag coefficient is $C_d = \frac{24}{\mathrm{Re}}(1 + 0.15\ \mathrm{Re}^{0.687})$. The magnitude of the magnetic field of the Nd magnet as a function of vertical position is fitted to an exponential function $|B_y| = 0.26 \exp(-192.9 \frac{1}{\mathrm{m}} y)$ T, where $y = 0$ corresponds to the surface of the magnet (0.26 T at the magnet's surface). As an interesting side note, the magnetic field strength to accelerate the bubble from the surface is higher than the one needed to keep the bubble neutrally buoyant. Probably it is the surface tension

which causes some activation energy in the separation of the shelled bubble from the free surface.

Figure 2(b) shows the trajectory of a bubble with a radius of 100 ± 10 μm. The continuous line represents the fit to the model using χ_b as the only free parameter. We find very good agreement between the measurement and the model over the whole observation time. The importance of the individual forces for this particular trajectory is shown in Fig. 2(c) as a function of time. As expected the added mass force contributes only at the very late stage, when the bubble is close to the magnet. The strong dependence of the modeled trajectory on χ_b gives us confidence to determine the parameter through the fitting procedure. This has been done for different bubble sizes, and the result is reported in Fig. 2(d). The bubble's susceptibility is proportional to the square of the radius $\chi_b = (9 \pm 3 \times 10^{-6}\ \mathrm{m}) r^2$. This agrees with the observation that the self-assembled magnetic nanoparticles form a thin shell around the bubble. It implies that the shell thickness is approximately constant for the range of bubble sizes studied. Let us now compare the measured susceptibility with the one expected from a spherical shell of magnetic material. The dimensionless susceptibility $\chi_m = 22.16$ of the Fe_3O_4 nanoparticles used in the recipe can be calculated from the magnetic dipole moment measured from the hysteresis curves of a sample of nanoparticles (averaged radius $r_p = 15$ nm) [18]. The susceptibility of a spherical shell is $\chi_b = V_{\mathrm{shell}} f(\chi_m)$, where V_{shell} is its volume and $f(\chi_m)$ is a function of the dimensionless susceptibility χ_m given, for example, in Ref. [19]. Assuming a constant shell thickness of 880 nm we obtain $\chi_b = (0.8\text{–}11.7) \times 10^{-14}\ \mathrm{m}^3$ for bubbles with radii from $r = 30$ μm to $r = 100$ μm. These numerical values agree nicely with the susceptibility obtained from the force balance method $\chi_b = (0.8 \pm 0.3\text{–}9 \pm 3) \times 10^{-14}\ \mathrm{m}^3$; see Fig. 2(d) considering the uncertainty in the shell thickness.

To study the compressibility of the magnetic shell, the bubbles are exposed to an alternating pressure field. A single bubble is placed in an acoustic container as shown in Fig. 3(a). At the closed end of the cuvette a piezotransducer (made of lead zirconate titanate material, a cylinder with a 10 mm diameter and a thickness of 5.5 mm) is attached, and the opposite side is sealed such that residual air pockets are avoided. As the cuvette is placed on its side, the bubble rises and makes contact with the top wall while retaining its mostly spherical shape. The transducer is driven with a sinusoidal voltage from a function generator connected to an amplifier and a voltage transformer. These magnetic bubbles oscillate when the frequency of the applied sound field is close to the bubble's resonance frequency. Figure 3(b) shows the shell oscillation of a bubble with a radius of 121 μm driven at 27 kHz. The bubble radius was extracted from images taken with a high-speed camera at 200, 000 frames/s. The bubble contour is then fitted to a circle and its radius extracted. We find peak-to-peak variations in the bubble radius of about 1.7 μm [20].

It is well known that oscillating bubbles induce a microstreaming flow [21–23]. To visualize the flow, microparticles are added to the liquid, and as soon as the acoustic field is switched on, we observe a microstreaming flow created by the oscillating bubble. Figure 4(a) depicts the flow pattern reconstructed with particle image velocimetry. In particular we find a vortex ring surrounding the upper pole of the bubble very similar to the observation of Marmottant and Hilgenfeldt [24], yet the magnetic bubble remains spherical due to the stiff shell. When the sound field is turned off, the induced recirculating flow stops instantaneously. Then the bubble is repositioned with an external magnet [Fig. 4(b)]. Flow visualization exhibits a background flow which resembles a stagnation point flow. After switching on the sound field [Fig. 4(c)], the bubble-induced flow pattern appears again. This demonstrates that the bubble's acoustic property has not been altered. The shell is stable despite the volume oscillations and magnetic manipulation.

In summary we report on the physical properties of magnetic shelled bubbles prepared with a simple recipe.

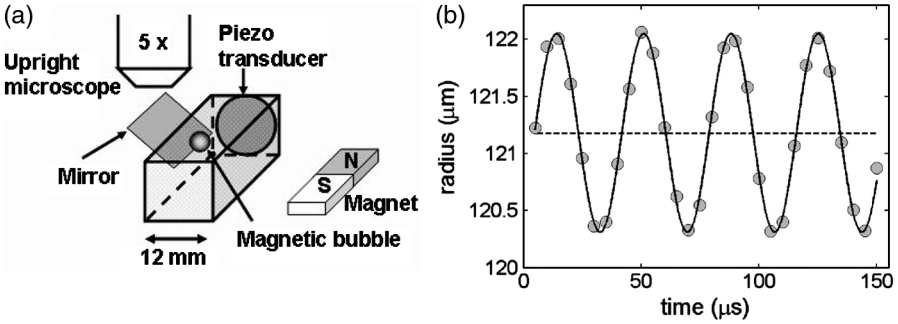

FIG. 3. (a) Experimental setup to study bubble shell oscillations. A polystyrene cuvette with a square cross section (12 mm width and 45 mm length) is viewed with a microscope from the side through a mirror. The bubble located at the top is driven into volume oscillations with an acoustic field generated from a piezoelectric device glued to the back of the cuvette. (b) High-speed recordings taken at 200, 000 frames/s exhibit the bubble radius as a function of time (circles) which is fitted to a sine (solid line); the driving frequency is 27 kHz.

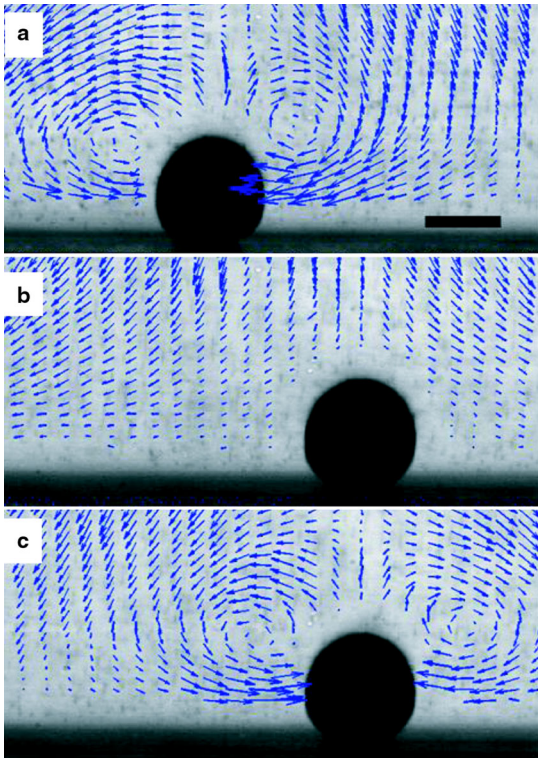

FIG. 4 (color online). (a) Magnetic bubble-induced microstreaming. A single magnetic bubble is excited with an acoustic field which creates a streaming flow. The flow pattern is visualized with 3 μm diameter polystyrene particles added to the liquid. The flow velocities are estimated by cross correlating parts of consecutive frames (particle image velocimetry) of the movie taken at 16.2 frames/s. At resonance a vortex ring is created at the bubble's upper pole. (b) The sound field is switched off, and the bubble is repositioned to the right using a permanent magnet. A residual stagnation type flow pattern remains. (c) The sound field (same amplitude and frequency) is switched on giving way to a very similar flow pattern translated to the right. The length of the scale bar is 100 μm.

The bubbles cover a broad range of sizes with radii ranging from 20 μm to 175 μm; they are exceptionally stable in gas-saturated liquids for many months. Their motion in a magnetic field has been successfully modeled with a force balance. Magnetic bubbles in contrast to magnetic emulsions [25] and colloidosomes [26] offer the advantage of being able to perform volume oscillations which, for example, can drive a microstreaming flow or create locally shear stresses. We expect that magnetic bubbles may offer novel solutions for microfluidics using two independent force fields, for example, exploiting stable bubbles as remotely controlled mixers and pumps, or for the stimulation of cells with spatially and temporally controlled hydrodynamic forces.

We acknowledge material support from Professor Helseth and financial support through Nanyang Technological University (RG39/07) and The Ministry of Education (ARC7/05), Singapore.

[1] C. D. Ohl, M. Arora, R. Dijkink, V. Janve, and D. Lohse, Appl. Phys. Lett. **89**, 074 102 (2006).
[2] K. S. Suslick, Science **247**, 1439 (1990).
[3] W. B. McNamara, Y. T. Didenko, and K. S. Suslick, Nature (London) **401**, 772 (1999).
[4] K. Wei, A. R. Jayaweera, S. Firoozan, A. Linka, D. M. Skyba, and S. Kaul, Circulation **97**, 473 (1998).
[5] P. N. Burns, S. R. Wilson, and D. H. Simpson, Investigative Radiology **35**, 58 (2000).
[6] T. K. Kim, B. I. Choi, J. K. Han, H. S. Hong, S. H. Park, and S. G. Moon, Radiology (Oak Brook, Ill.) **216**, 411 (2000).
[7] E. C. Unger, T. Porter, W. Culp, R. Labell, T. Matsunaga, and R. Zutshi, Adv. Drug Delivery Rev. **56**, 1291 (2004).
[8] T. L. Li, K. Tachibana, M. Kuroki, and M. Kuroki, Radiology (Oak Brook, Ill.) **229**, 423 (2003).
[9] K. Soetanto and H. Watarai, Jpn. J. Appl. Phys. **39**, 3230 (2000); F. Yang, A. Gu, Z. Chen, N. Gu, and M. Ji, Mater. Lett. **62**, 121 (2008).
[10] T. G. Leighton, *The Acoustic Bubble* (Academic Press, London, 1997).
[11] M. P. Brenner, S. Hilgenfeldt, and D. Lohse, Rev. Mod. Phys. **74**, 425 (2002).
[12] J. B. Young, T. Schmiedel, and W. Kang, Phys. Rev. Lett. **77**, 4816 (1996).
[13] M. Tada, S. Hatanaka, H. Sanbonsugi, N. Matsushita, and M. Abe, J. Appl. Phys. **93**, 7566 (2003).
[14] O. A. Sapozhnikov, V. A. Khokhlova, M. R. Bailey, J. C. Williams, J. A. McAteer, R. O. Cleveland, and L. A. Crum, J. Acoust. Soc. Am. **112**, 1183 (2002).
[15] M. A. M. Gijs, Microfluid. Nanofluid. **1**, 22 (2004).
[16] C. D. Ohl, A. Tijink, and A. Prosperetti, J. Fluid Mech. **482**, 271 (2003).
[17] R. Clift, J. R. Grace, and M. E. Weber, *Bubbles, Drops, and Particles* (Academic Press, New York, 1978).
[18] X. Zhao and L. E. Helseth, J. Appl. Phys. **102**, 054 905 (2007).
[19] J. D. Jackson, *Classical Electrodynamics* (John Wiley & Sons, New York, 1998).
[20] Preliminary experiments show that although the bubble oscillations are reduced by the magnetic shell, the amplitude is of the same order of magnitude as for a free bubble. The stiffening of the shell will give a higher resonance frequency for the magnetic bubble.
[21] J. Lighthill, J. Sound Vib. **61**, 391 (1978).
[22] M. S. Longuet-Higgins, Proc. R. Soc. A **454**, 725 (1998).
[23] P. Marmottant, J. P. Raven, H. Gardeniers, J. G. Bomer, and S. Hilgenfeldt J. Fluid Mech. **568**, 109 (2006).
[24] P. Marmottant and S. Hilgenfeldt, Nature (London) **423**, 153 (2003).
[25] S. Melle, M. Lask, and G. G. Fuller, Langmuir **21**, 2158 (2005).
[26] H. Duan, D. Wang, N. S. Sobal, M. Giersig, D. G. Kurth, and H. Mohwald, Nano Lett. **5**, 949 (2005).